Journal of Magnetic Resonance **149,** 29–35 (2001)
doi:10.1006/jmre.2000.2268, available online at http://www.idealibrary.com on IDEAL®

Automatic Coupling Control of a Loop–Gap Resonator by a Variable Capacitor Attached Coupling Coil for EPR Measurements at 650 MHz

Hidekastu Yokoyama,[1] Toshiyuki Sato,* Tateaki Ogata,† Hiroaki Ohya, and Hitoshi Kamada

*Institute for Life Support Technology, 2-2-1 Matsuei, Yamagata 990-2473, Japan; *Yamagata Research Institute of Technology, 2-2-1 Matsuei, Yamagata 990-2473, Japan; and †Graduate School of Science and Engineering, Yamagata University, 4-3-16 Jonan, Yonezawa 992-8510, Japan*

Received July 31, 2000; revised November 14, 2000

A coupling coil was fabricated that can electrically change the magnetic coupling with a loop–gap resonator (LGR) for EPR studies at 650 MHz. It is composed of a single-turn coil and a coupling control circuit that includes a varactor diode. The coarse control of the magnetic coupling is made by mechanically changing the distance between the LGR and single-turn coil. The fine control is obtained by changing the capacitance of the varactor diode that is connected in parallel with the single-turn coil. This capacitance is controlled by changing reverse voltage from a variable bias voltage source. Because this can be located far from the resonator, remote control of coupling of the LGR is possible. Automatic coupling control (ACC) was accomplished by negative feedback of the DC component in the radiowaves reflected from the LGR to the coupling control circuit when the LGR was irradiated precisely at its resonant frequency. To accomplish this, automatic frequency control (AFC) is used. In EPR measurements of a phantom that included a physiological saline solution containing a nitroxide radical, it was confirmed that the drifts in the coupling and resonant frequency caused by the perturbation of the resonant nature could be sufficiently compensated by the ACC and AFC systems. In the *in vivo* EPR studies, it was found that the deviation of coupling at the chest of a mouse is greater than that at the head of a rat, but the ACC system could compensate for the respiratory motions of a living animal.

Key Words: **loop–gap resonator; coupling coil; automatic coupling control; automatic frequency control; *in vivo* EPR.**

INTRODUCTION

A loop–gap resonator (LGR) (*1–3*), one of the frequently used EPR resonators for *in vivo* study (*4–6*), is coupled to the external circuits by one of two methods: capacitive or magnetic coupling (*7*). To obtain EPR spectra with a good signal-to-noise ratio (SNR), it is necessary to control the coupling to minimize reflections from the resonator. With the capacitive coupling technique, coupling of the LGR is controlled by electrically changing the capacitance between the RF transmission line and the LGR. With the magnetic coupling technique, coupling is controlled by mechanically changing the distance between the coupling coil and the LGR. Automatic coupling control (ACC) was electrically accomplished by using a varactor diode (*8*) or a piezoelectric-controlled capacitor (*9*) in the first method. In the second method, a mechanically driven ACC was also achieved by using a coupling coil (*10*). However, electrical ACC by using a coupling coil has not been attempted. In this study, a coupling coil was newly developed to permit electrical control of the magnetic coupling to the LGR. By using this coil, it became possible to employ ACC to make EPR measurements of a phantom and a living rat or mouse.

[1] To whom correspondence should be addressed. E-mail: yokohide@fmu.ac.jp.

RESULTS AND DISCUSSION

Coupling Coil

Our coupling coil was composed of a single-turn coil and coupling control circuit (Fig. 1). The inner diameter of the single-turn coil, which was constructed from copper wire measuring 1 mm in diameter, was 40 mm. The coil was connected to the coupling control circuit via a quarter wavelength parallel transmission line (*11*).

A description of the coupling control circuit follows. A varactor diode (1SV153, Toshiba, Japan; *D* in Fig. 1) in series with a fixed capacitor (C_1 in Fig. 1) is connected to the single-turn coil in parallel. This varactor diode, which has a capacitance that varies from 16.25 pF at a reverse voltage of 2 V to 2.43 pF at 25 V, is mainly used for the electric tuning in the VHF and UHF bands (*12*). The fixed capacitor prevents the DC current from flowing into the single-turn coil when a DC reverse voltage is applied to the varactor. When the capacitance of the fixed capacitor is smaller than that of the varactor, most of the RF voltage is applied to the fixed capacitor, which means that the varactor will be protected from high RF power. Under this condition, the varactor contributes a smaller proportion of the total capacitance: thus it is suitable as a means to provide fine control of the coupling. The capacitance of the varactor diode was set around 10 pF and a 3-pF ceramic capacitor was used as the fixed capacitor.

A DC reverse voltage is applied to the varactor by a bias voltage source, via an inductor (*L* in Fig. 1) and a resister (*R* in Fig. 1). The inductor (air core coil, 70 nH) and resister (3.3 kΩ) prevent leakage of the RF current. The resistance of the resister

1090-7807/01 $35.00

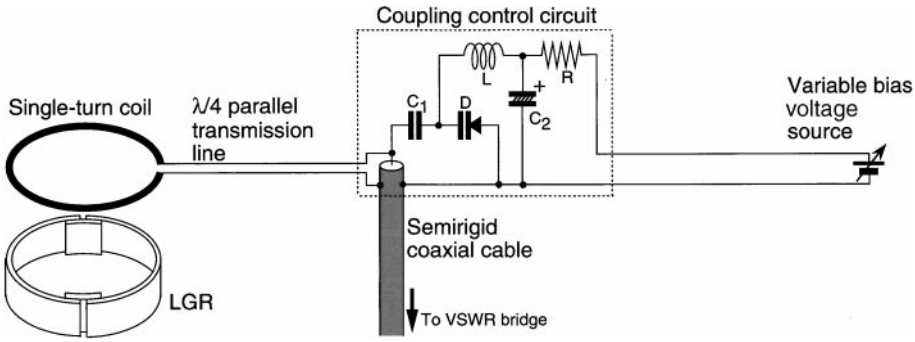

FIG. 1. Schematic diagram of the LGR and the coupling coil which is composed of a single-turn coil and a coupling control circuit. A varactor diode (D) in series with a fixed capacitor (C_1) is connected to the single-turn coil in parallel. A reverse voltage is applied to the varactor diode by a bias voltage source via an inductor (L) and resistor (R). This resisitor, together with a fixed capacitor (C_2), also serves as an RC circuit. The values of C_1, C_2, L, and R are 3 pF, 10 μF, 70 nH, and 3.3 kΩ, respectively.

is sufficiently large compared to the impedance of the varactor at the resonant frequency of the LGR. This resister also serves as an *RC* circuit (time constant, 33 ms) with a fixed capacitor (tantalum electrolytic capacitor, 10 μF; C_2 in Fig. 1), which protects the varactor from the voltage disturbance at a field modulation frequency of 100 kHz.

The magnetic coupling is roughly controlled by mechanically changing the distance between the LGR and the single-turn coil. The fine control is achieved by changing the capacitance of the varactor diode that is connected in parallel to the single-turn coil. This capacitance is controlled by changing reverse voltage from the variable bias voltage source. Figure 2 shows an example of the fine control of the coupling of a phantom containing a nitroxide radical solution in the LGR. Because the bias voltage source can be located far from the resonator, remotely controlling the LGR coupling is possible.

Automatic Frequency Control and Automatic Coupling Control Systems

Figure 3 shows a block diagram of the EPR spectrometer that was used in this study. ACC was accomplished by negative feedback of the DC component of the radiowaves reflected from the LGR to the coupling control circuit when the LGR was irradiated at a precise resonant frequency. To do this, automatic frequency control (AFC) is needed.

A description of the AFC circuit follows (see Fig. 3). The rectified signals from the double balance mixer are amplified and applied to the AFC input. The RF is modulated at an AFC frequency of 70 kHz. The AFC signal is detected by a lock-in amplifier (5210, PARC; frequency range, 0.5 Hz–120 kHz) at the AFC frequency. The output of the lock-in amplifier is summed with the AC component, which is generated by an internal oscillator in the lock-in amplifier at the AFC frequency. The amplitude of the AC component regulates the FM depth of the RF source. The summing amplifier is implemented with a stable unity gain and high speed (LM 6361, National Semiconductor, Santa Clara) (*13*). The output of the summing amplifier (i.e., AFC output) is applied to the DC FM input of the RF source to shift the RF. The DC potential of the AFC output produces an offset that corrects for the frequency drift in the LGR. The AFC ON/OFF switch is located between the output of the lock-in amplifier and the summing amplifier. When the basic frequency of

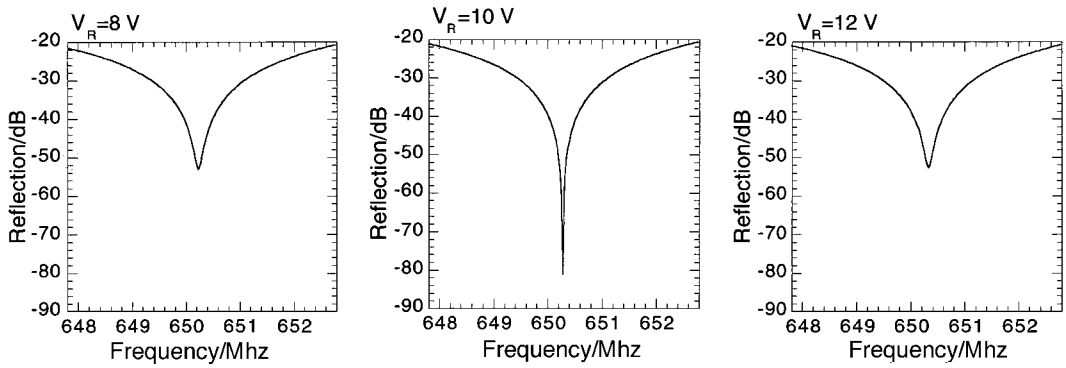

FIG. 2. An example of fine control of the coupling of a phantom containing 10 ml of a 1 mM solution of carbamoyl-PROXYL that had been dissolved in a physiological saline solution. The reflections from the LGR were measured by employing a network analyzer (8714C, Hewlett–Packard, Palo Alto; bandwidth, 0.3–3000 MHz) when a reverse voltage of 8, 10, and 12 V was applied to the varactor diode.

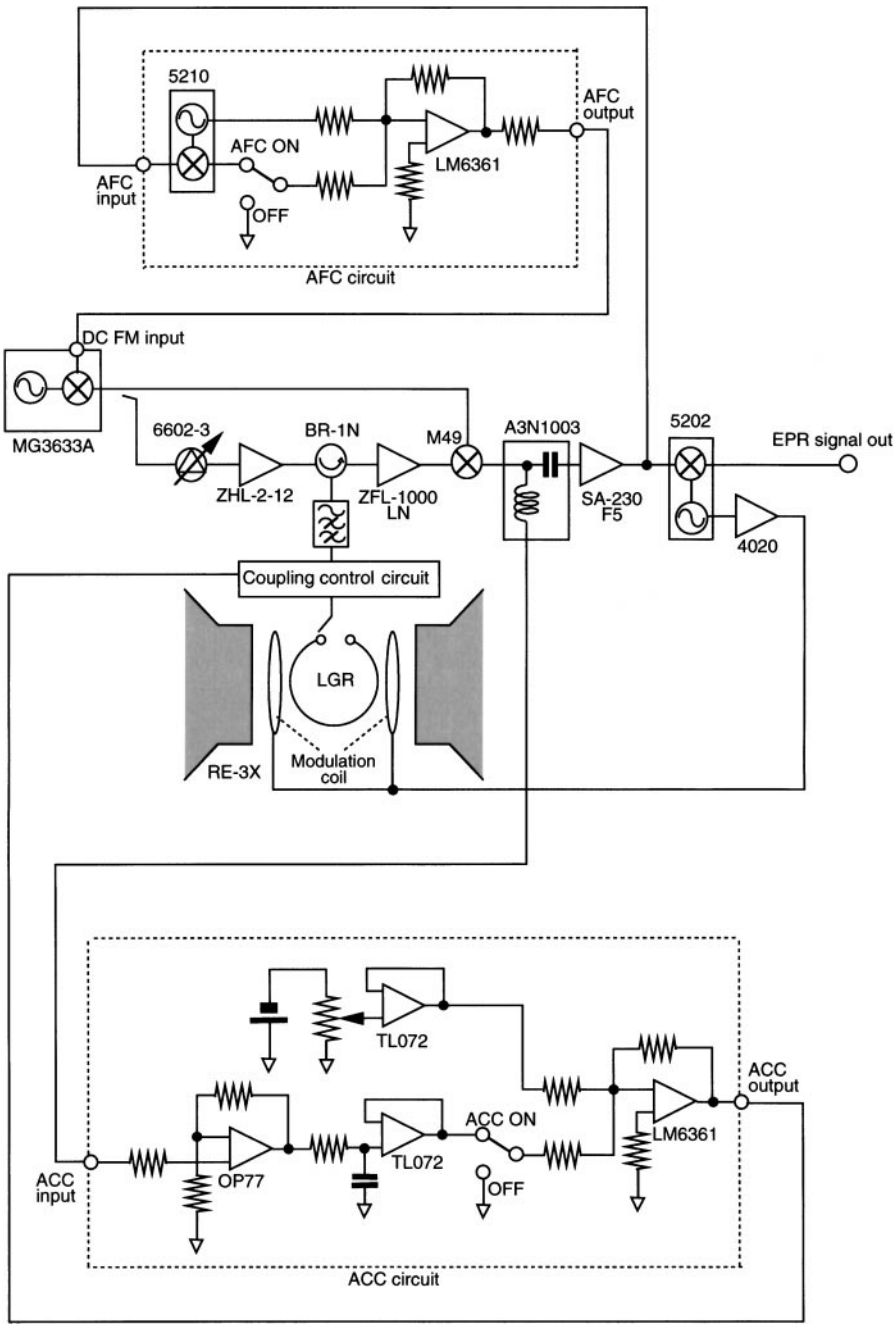

FIG. 3. Block diagram of our EPR spectrometer, including AFC and ACC systems. For the main magnet, a modified RE3X was used. MG3633A was used as an RF source for EPR excitation. The RF circuit for EPR detection was constructed with a power amplifier (ZHL-2-12), a VSWR bridge (BR-1N), a phase shifter (6602-3), a preamplifier (ZFL-1000LN), and a double balance mixer (M49) for homodyne detection. The rectified signals were amplified by SA-230F5 and detected by a lock-in amplifier (5202) at a magnetic field modulation frequency of 100 kHz. A pair of modulation coils was driven by an internal oscillator in 5202 and a power amplifier (4020) at 100 kHz. The RF was modulated at an AFC frequency of 70 kHz. The rectified radiowave was applied to the AFC input. The AFC signal was detected by a lock-in amplifier (5210). The output of 5210 was summed (LM6361) with the AC component which was generated by an internal oscillator in 5210 at 70 kHz. The output of LM6361 (AFC output) was applied to the DC FM input of MG3633A to shift the RF. The DC component in the rectified radiowave was obtained from a bias T-connector (A3N1003) and applied to the ACC input. The ACC signal was preamplified by OP-77, went through an RC circuit, and was buffered (TL072). The buffer output was summed (LM 6361) with the DC offset from the various bias voltage source (including TL072). The output of LM6361(ACC output) was applied to the coupling control circuit.

the RF source is changed (up to a 1-MHz difference) under AFC in the EPR measurement of the phantom, the summed basic and FM offset frequency are stable. This indicates that the feedback loop of the AFC circuit is working with a sufficient loop gain.

The ACC is described next (see Fig. 3). The DC component of the rectified signals from the double balance mixer (i.e., ACC signal), which is obtained by employing a bias T-connector (A3N1003, Anritsu; frequency range, 100 kHz–20 GHz), is applied to the input of the ACC circuit. The ACC signal is preamplified by a high-precision operational amplifier (OP-77, Analog Devices, Norwood) (*14*). The output of the preamplifier goes through an *RC* circuit (time constant, 10 ms), is buffered (TL072, Texas Instruments, Dallas) (*15*), and is summed (LM 6361) with the DC offset from the various bias voltage source, which is constructed by a stable bias voltage source, an operational amplifier (TL072), and a variable resistor. The output of the summing amplifier (i.e., ACC output) is applied to the coupling control circuit. The ACC output produces an offset that corrects for the coupling drift in the LGR. The ACC ON/OFF switch is located between the output of the buffer and the summing amplifier. When the voltage of the bias voltage source is changed (up to a 5-V difference) under ACC and AFC in the EPR measurement of the phantom, the ACC output to the coupling control circuit is stable. This indicates that the ACC feedback loop is operating with a sufficient loop gain.

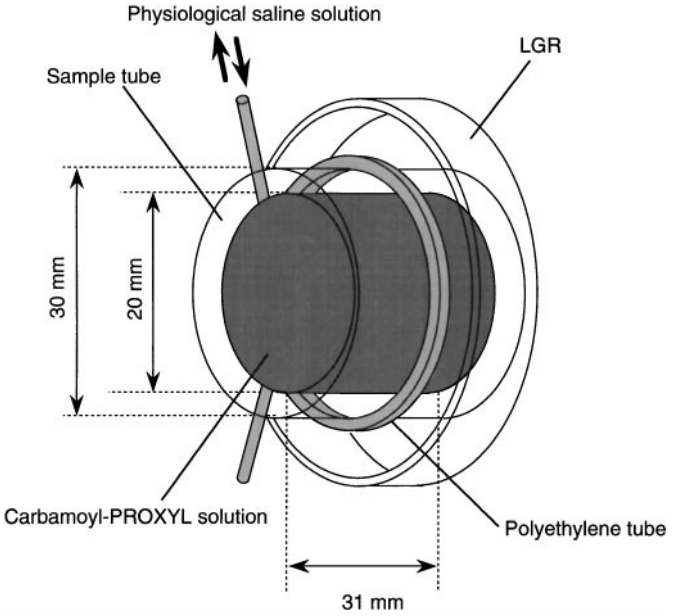

FIG. 4. Schema of the phantom and two-turn coil-shaped polyethylene tube in the LGR for perturbation of the resonant natures. The phantom is a sample tube that holds 10 ml of physiological saline solution containing 1 mM carbamoyl-PROXYL. The polyethylene tube is placed outside the phantom. When the resonant natures are perturbed, the physiological saline solution is pushed into the tube in the LGR. When the perturbation ceases, the physiological saline solution is drained from the tube.

EPR Measurements of a Phantom, Rat, and Mouse

The involvement of ACC and AFC against perturbation of resonant natures was verified in a phantom study. The resonant natures were perturbed by the inflow of a physiological saline solution into a two-turn coil-shaped polyethylene tube placed outside the phantom, which contained a nitroxide radical solution in the LGR (Fig. 4).

Figure 5 shows examples of EPR spectra before and after the perturbation. The loaded *Q* values before and after the perturbation were 80 and 74, respectively. Under this condition, the resonant frequency was 651.6 or 651.0 MHz. Before perturbation, both ACC and AFC were ON (Fig. 5a). After perturbation, EPR measurements were conducted without retuning under the following four different conditions: ACC-ON and AFC-ON (Fig. 5b); ACC-OFF and AFC-ON (Fig. 5c); ACC-ON and AFC-OFF (Fig. 5d); and ACC-OFF and AFC-OFF (Fig. 5e). The measurements were also made after perturbation and retuning (Fig. 5f).

Table 1 shows the signal and noise intensity for each condition before and after perturbation. The signal intensity is derived from peak-to-peak height of the lowest component in the triplet spectrum. The noise intensity is represented by rms noise. Values are means ± standard deviation of output voltage of the lock-in amplifier from five independent determinations. When the resonant natures were perturbed with ACC- and AFC-ON without retuning, the signal intensity was slightly reduced (about by 5%) and the noise intensity remained (within the margin of error). However, the signal and noise intensities after perturbation and retuning were almost the same as those with ACC- and AFC-ON without retuning after perturbation (within the margin of error). These findings indicate that the drifts in the coupling and resonant frequency caused by the perturbation of the resonant nature was adequately compensated by the ACC and AFC systems.

When ACC was turned off after perturbation, the signal intensity was reduced by about 40% and the noise intensity increased by about 40%, in comparison with those when ACC- and AFC-ON, indicating that sensitivity is impaired by perturbation without ACC. When AFC was turned off after perturbation, the signal intensity was reduced by about 30% and the noise

TABLE 1
The Signal and Noise Intensities of the EPR Spectra of the Phantom before and after Perturbation

Perturbation	Retuning	ACC	AFC	Signal intensity/mV	Noise intensity/mV
−	−	+	+	8.779 ± 0.063	0.042 ± 0.002
+	−	+	+	8.210 ± 0.051	0.042 ± 0.004
+	−	−	+	5.178 ± 0.160	0.058 ± 0.004
+	−	+	−	6.212 ± 0.073	0.148 ± 0.033
+	−	−	−	4.747 ± 0.093	0.064 ± 0.005
+	+	+	+	8.195 ± 0.055	0.042 ± 0.004

Note. Values are means ± standard deviation of the output voltage of the lock-in amplifier from five independent determinations.

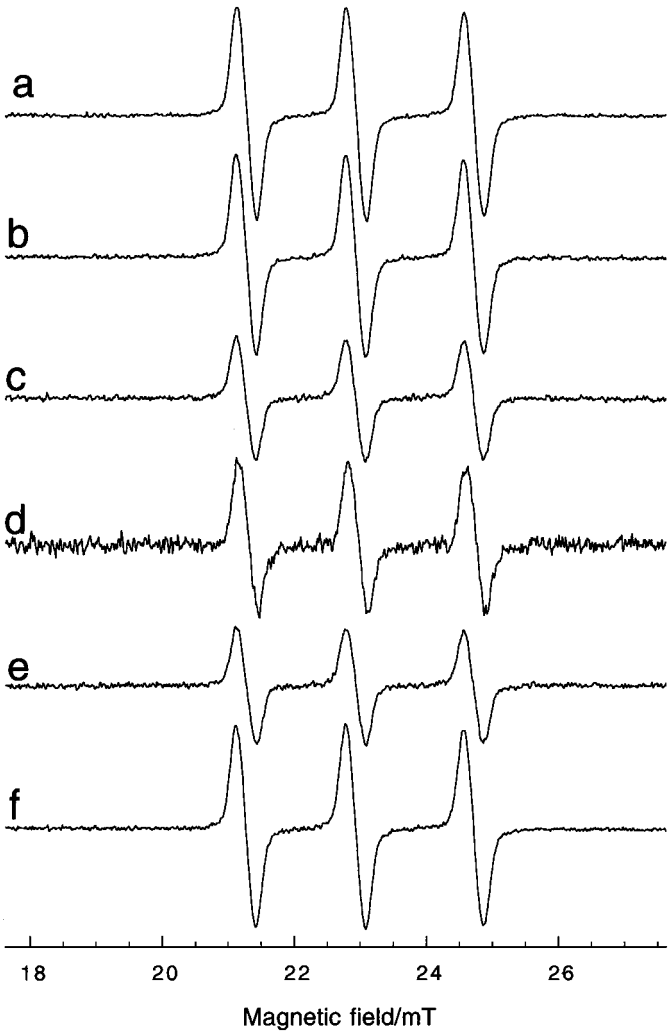

FIG. 5. Examples of EPR spectra of the phantom before and after perturbation. Before perturbation, both ACC and AFC were on (a). After perturbation, EPR measurements were conducted without retuning under the following four conditions: ACC-ON and AFC-ON (b); ACC-OFF and AFC-ON (c); ACC-ON and AFC-OFF (d); and ACC-OFF and AFC-OFF (e). The measurements were also made after perturbation and retuning (f). The EPR conditions were RF power, 80 mW; resonant frequency, 651.6 (a, d, and e) or 651.0 MHz (b, c, and e); scan rate, 5 mT/s; accumulation number, 2; field modulation width 0.2 mT at 100 kHz; time constant, 1 ms.

intensity increased markedly (by about 250%), in comparison with that at ACC- and AFC-ON. Because the irradiation to the LGR at a precise resonant frequency is disabled in the absence of AFC, the ACC circuit gives incorrect feedback to the coupling control circuit. Thus it is thought that noise was markedly augmented with ACC-ON and AFC-OFF. When both ACC and AFC were turned off after perturbation, the signal intensity was reduced by about 50% and the noise intensity increased by about 50%, in comparison with ACC- and AFC-ON. When ACC- and AFC-ON were switched to ACC-OFF and AFC-ON, the SNR was reduced by about 60%; and when ACC-OFF and AFC-ON were switched to ACC- and AFC-OFF, the SNR was reduced

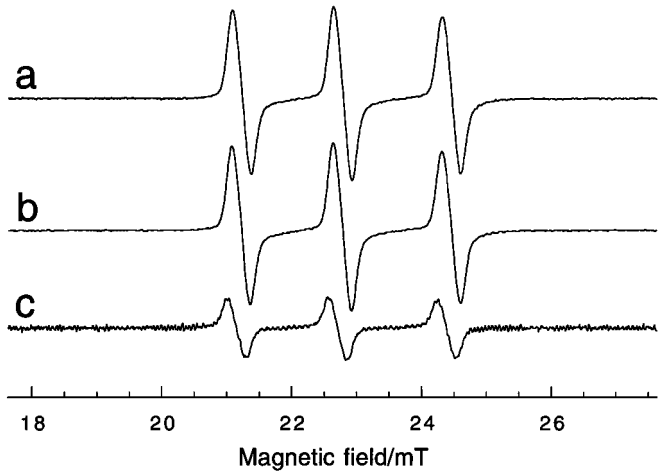

FIG. 6. Examples of EPR spectra at the head of an anesthetized rat. The EPR measurements were repeated under the following three conditions 15 min after administering the carbamoyl-PROXYL solution: ACC-ON and AFC-ON (a); ACC-OFF and AFC-ON (b); ACC-OFF and AFC-OFF (c). The resonant frequency was 647.5 (a and b) or 646.5 MHz (c). The other EPR conditions were same as those noted in the legend to Fig. 5.

by about 20%. Thus it was presumed that the influence of the drift in the coupling caused by the perturbation on the resonant nature is greater than that on the resonant frequency under the conditions in this study.

The influence of ACC and AFC in the *in vivo* studies at the head of a rat and the chest of a mouse was estimated. Figure 6 shows examples of EPR spectra from the head of a living, anesthetized rat. The EPR measurements were repeated five times under the following three different conditions 15 min after the administration of a nitroxide radical solution: ACC-ON and AFC-ON (Fig. 6a); ACC-OFF and AFC-ON (Fig. 6b); and ACC-OFF and AFC-OFF (Fig. 6c). The loaded Q value and resonant frequency were 46 and 647.5 MHz, respectively.

Table 2 shows the signal and noise intensity under each condition. When ACC was turned off, the signal intensity was slightly reduced (by about 5%), but the noise intensity did not change (within the margin of error) in comparison with those when ACC and AFC were on. When both ACC and AFC were turned off, the signal intensity was reduced by about 70% and the noise intensity increased by about 300%, in comparison with

TABLE 2
The Signal and Noise Intensities of the EPR Spectra at the Head of a Rat Treated with Carbamoyl-PROXYL

ACC	AFC	Signal intensity/mV	Noise intensity/mV
+	+	23.330 ± 0.170	0.050 ± 0.006
−	+	21.886 ± 0.504	0.045 ± 0.004
−	−	6.828 ± 1.089	0.177 ± 0.004

Note. Values are means ± standard deviation of the output voltage of the lock-in amplifier from five determinations.

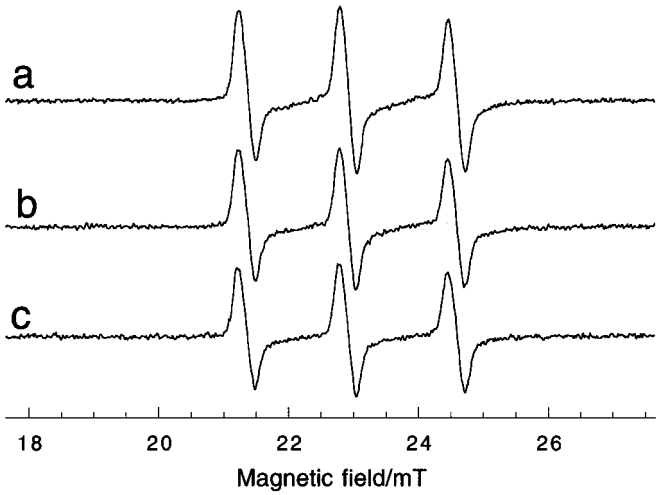

FIG. 7. Examples of EPR spectra at the chest of an anesthetized mouse. The EPR measurements were repeated under the following three conditions 15 min after administering the carbamoyl-PROXYL solution: ACC-ON and AFC-ON (a); ACC-OFF and AFC-ON (b); ACC-OFF and AFC-OFF (c). The resonant frequency was 650.8 (a and b) or 651.0 MHz (c). The other EPR conditions were same as those noted in the legend to Fig. 5.

those with ACC-OFF and AFC-ON. These findings suggest that deviations in coupling are negligible for the head of a rat under the conditions of this *in vivo* experiment.

Figure 7 shows examples of EPR spectra from the chest of a living, anesthetized mouse. The EPR measurements were repeated five times under the following three different conditions 15 min after the administration of a nitroxide radical solution: ACC-ON and AFC-ON (Fig. 7a); ACC-OFF and AFC-ON (Fig. 7b); and ACC-OFF and AFC-OFF (Fig. 7c). The loaded Q value and resonant frequency were 80 and 650.8 MHz, respectively.

Table 3 shows the signal and noise intensity under each condition. When ACC was turned off, the signal intensity was reduced by about 20% and the noise intensity increased by about 20% in comparison with those with ACC- and AFC-ON. When both ACC and AFC were turned off, the signal and noise intensities remained (within the margin of error), compared to those with ACC-OFF and AFC-ON. These findings suggest that deviations in coupling are not without an effect at the mouse's chest under the condition of this *in vivo* experiment. The extent of sample motion at the chest of the mouse is greater than that at the head of the rat. Thus it was presumed that the major benefit of an ACC system is in countering the effect of physiological motions in the *in vivo* experiment.

TABLE 3
The Signal and Noise Intensities of the EPR Spectra at the Chest of a Mouse Treated with Carbamoyl-PROXYL

ACC	AFC	Signal intensity/mV	Noise intensity/mV
+	+	8.541 ± 0.071	0.059 ± 0.004
−	+	7.015 ± 0.139	0.072 ± 0.008
−	−	6.875 ± 0.184	0.080 ± 0.021

Note. Values are means ± standard deviation of the output voltage of the lock-in amplifier from five determinations.

Because the time constant for the coupling control circuit is 30 ms, its cutoff frequency as a low-pass filter is estimated to be 4.8 Hz. The respiratory rate of an anesthetized mouse is about 2–3 times/s, which is near the estimated cutoff frequency. However, when ACC was turned on, the amplitude of the ACC signal oscillation caused by the respiratory motions of the mouse was reduced by more than 80%, and so it appears that the ACC system has a sufficient loop gain to compensate for the respiratory motion.

EXPERIMENTAL

LGR and EPR Spectrometer

The LGR used in this study is a two-gap type, with electric shields located inside the resonator (Fig. 1), which measures 41 mm in inner diameter and 10 mm in axial length. This resonator was driven at a frequency of approximately 650 MHz. The unloaded Q factor was 600.

For the main magnet, a commercially available electromagnet (modified RE3X, JEOL, Japan) was used; and for the field scan coils, a supplementary Helmholtz coil (Yonezawa electric wire, Japan) was employed. The magnetic field was scanned by controlling the current in the field scan coils at a maximum scan rate of 7.5 mT/s. A synthesized oscillator (MG3633A, Anritsu, Japan; frequency range, 10 kHz–2700 MHz; maximum width of FM, 1.6 MHz) was used as an RF source for EPR excitation. The RF circuit for EPR detection was constructed with a power amplifier (ZHL-2-12, Mini Circuit, New York; frequency range, 10–1200 MHz; gain, 24 dB); a VSWR bridge (BR-1N, Kuranishi, Japan; frequency range, 10–1300 MHz; insertion loss, 6.5 dB); a phase shifter (6602-3, Sage, Palo Alto; frequency range, DC-2 GHz; minimum phase shift, 290°/GHz); a preamplifier (ZFL-1000LN, Mini Circuit; frequency range, 0.1–1000 MHz; gain, 20 dB); and a double balance mixer (M49, R&K, Japan; frequency range, 1–2000 MHz) for homodyne detection. The rectified signals were amplified by a low-noise amplifier (SA-230F5, NF, Japan; gain 46 dB; frequency range, 1 kHz–100 MHz; noise figure, 0.6 dB) and detected by a lock-in amplifier (5202, PARC, Princeton; frequency range, 1 mHz–1 MHz) at the magnetic field modulation frequency. A pair of modulation coils (inner diameter, 46 mm; outer diameter, 68 mm; 40 turns; distance between coils, 66 mm) was driven by an internal oscillator in the lock-in amplifier and a power amplifier (4020, NF, Japan; gain, 46 dB) at 100 kHz (Fig. 3).

Phantom

Ten milliliters of a 1 mM solution of a nitroxide radical, 3-carbamoyl-2,2,5,5-tetramethylpyrrolidin-1-yloxy (carbamoyl-PROXYL, Aldrich Chem. Co., Ltd., Milwaukee), which had

been dissolved in a physiological saline solution (a 0.9% sodium chloride aqueous solution), was placed in a sample tube (inner diameter, 20 mm; axial length, 31 mm) for use as a phantom.

For perturbation of the resonant natures, a two-turn coil-shaped polyethylene tube (inner diameter, 0.75 mm; outer diameter, 1.5 mm) was placed outside the phantom. When the resonant natures are perturbed, the physiological saline solution is pushed into the tube in the LGR. When the perturbation ceases, the physiological saline solution is drained from the tube (Fig. 4).

Animals

Carbamoyl-PROXYL was dissolved in a physiological saline solution at 0.2 M. A male Wistar rat weighing 180 g or a ddy mouse weighing 50 g received 5 ml (1 mmol) or 0.5 ml (0.1 mmol) of a carbamoyl-PROXYL solution via the intraperitoneal route, respectively. Ten minutes after the injection and under pentobarbital anesthesia (37.5 mg/kg, injected intraperitoneally), the animal was inserted into the LGR. The head of the rat was located with its interaural line aligned 7 mm posterior to the center of the resonator. The chest of the mouse was located with its xyphoid process aligned 10 mm posterior to the center of the resonator.

REFERENCES

1. W. Froncisz and J. S. Hyde, *J. Magn. Reson*. **47,** 515 (1982).
2. M. Ono, T. Ogata, K. Hsieh, M. Suzuki, E. Yoshida, and H. Kamada, *Chem. Lett.*, 491 (1986).
3. H. Hirata and M. Ono, *Rev. Sci. Instrum*. **67,** 73 (1996).
4. S. Ishida, S. Matsumoto, H. Yokoyama, N. Mori, H. Kumashiro, N. Tsuchihashi, T. Ogata, M. Yamada, M. Ono, T. Kitajima, H. Kamada, and E. Yoshida, *Magn. Reson. Imaging* **10,** 21 (1992).
5. H. Yokoyama, T. Ogata, N. Tsuchihashi, M. Hiramatsu, and N. Mori, *Magn. Reson. Imaging* **14,** 559 (1996).
6. H. Yokoyama, T. Sato, T., Ogata, H. Ohya-Nishiguchi, and H. Kamada, *J. Magn. Reson.* **129,** 201 (1997).
7. G. A. Rinard, R. W. Quine, S. S. Eaton, and G. R. Eaton, *J. Magn. Reson*. **105,** 137 (1993).
8. H. J. Halpern, D. P. Spencer, J. Polen, M. K. Bowman, A. C. Nelson, E. M. Dowey, and B. A. Teicher, *Rev. Sci. Instrum*. **60,** 1040 (1989).
9. S. McCallum and F. Resmer, *Rev. Sci. Instrum*. **70,** 4706 (1999).
10. J. A. Brivati, A. D. Stevens, and M. C. R. Symons, *J. Magn. Reson*. **92,** 480 (1991).
11. H. Hirata, T. Walcak, and H. M. Swartz, *Rev. Sci. Instrum*. **68,** 3187 (1997).
12. "The Diode Manual," p. 192, CQ Shuppan, Tokyo (1995).
13. "Linear Databook," p. 2-492–503, National Semiconductor, Santa Clara (1988).
14. "Linear Databook," p. 4-654–665, Analog Devices, Norwood (1988).
15. "Linear Circuit Databook," p. 7-99–106, Texas Instruments, Dallas (1988).